THE JOURNAL OF BIOLOGICAL CHEMISTRY
Vol. 277, No. 26, Issue of June 28, pp. 23150–23156, 2002
Printed in U.S.A.

Activation of the Cation Channel Long Transient Receptor Potential Channel 2 (LTRPC2) by Hydrogen Peroxide

A SPLICE VARIANT REVEALS A MODE OF ACTIVATION INDEPENDENT OF ADP-RIBOSE*

Received for publication, December 18, 2001, and in revised form, March 18, 2002
Published, JBC Papers in Press, April 17, 2002, DOI 10.1074/jbc.M112096200

Edith Wehage‡, Jörg Eisfeld‡, Inka Heiner, Eberhard Jüngling, Christof Zitt§, and Andreas Lückhoff¶

From the Institute of Physiology, Medical Faculty, Rheinisch-Westfälische Technische Hochschule Aachen, Pauwelsstrasse 30, D-52057 Aachen, Germany

LTRPC2 is a cation channel recently reported to be activated by adenosine diphosphate-ribose (ADP-ribose) and NAD. Since ADP-ribose can be formed from NAD and NAD is elevated during oxidative stress, we studied whole cell currents and increases in the intercellular free calcium concentration ($[Ca^{2+}]_i$) in *long transient receptor potential channel 2* (*LTRPC2*)-transfected HEK 293 cells after stimulation with hydrogen peroxide (H_2O_2). Cation currents carried by monovalent cations and Ca^{2+} were induced by H_2O_2 (5 mM in the bath solution) as well as by intracellular ADP-ribose (0.3 mM in the pipette solution) but not by NAD (1 mM). H_2O_2-induced currents developed slowly after a characteristic delay of 3–6 min and receded after wash-out of H_2O_2. $[Ca^{2+}]_i$ was rapidly increased by H_2O_2 in *LTRPC2*-transfected cells as well as in control cells; however, in *LTRPC2*-transfected cells, H_2O_2 evoked a second delayed rise in $[Ca^{2+}]_i$. A splice variant of LTRPC2 with a deletion in the C terminus (amino acids 1292–1325) was identified in neutrophil granulocytes. This variant was stimulated by H_2O_2 as the wild type. However, it did not respond to ADP-ribose. We conclude that activation of LTRPC2 by H_2O_2 is independent of ADP-ribose and that LTRPC2 may mediate the influx of Na^+ and Ca^{2+} during oxidative stress, such as the respiratory burst in granulocytes.

The long transient receptor potential channel 2 (LTRPC2)[1] is a member of the transient receptor potential (TRP) family of cation channels (1). Its function may not be confined to that of a Ca^{2+}-permeable ion channel widely expressed in several cell types but may extend to the role of an enzyme, as has been shown for its relative TRP-phospholipase C interacting kinase (2). LTRPC2 contains a Nudix box in its C terminus (3) which is a common motif of enzymes degrading mostly nucleoside diphosphates (4). The protein NUDT9 that is homologous to the C terminus of LTRPC2 is a specific ADP-ribose pyrophosphatase degrading ADP-ribose (3). A similar function may be attributed to LTRPC2. Alternatively, the Nudix box may serve as a regulatory ADP-ribose-binding site because ADP-ribose has been shown to stimulate the channel activity of LTRPC2 (3). Therefore, ADP-ribose can be thought of as a novel second messenger regulating Ca^{2+} influx. However, the stimuli and signaling pathways leading to elevated levels of ADP-ribose have not been elucidated in detail. ADP-ribose can be generated from cyclic ADP-ribose (5–7), an established messenger mobilizing Ca^{2+} from ryanodine-sensitive calcium stores (8–12). Moreover, ADP-ribose can be produced from NAD (13, 14). This links ADP-ribose to the redox state of the cell and may lead to the assumption that ADP-ribose and ADP-ribose-induced Ca^{2+} influx play a role during oxidative stress because a characteristic feature of oxidative stress is an increased ratio of NAD to NADH (15). In this context, it is of interest that NAD has been reported to be a further stimulus of LTRPC2 channels (16, 17).

To study the role of LTRPC2 in oxidative stress, we used an experimental model in which a strong oxidant, H_2O_2, was applied to *LTRPC2*-transfected cells. Indeed, H_2O_2 evoked cation influx and increased $[Ca^{2+}]_i$. Furthermore, we studied the effects of H_2O_2 on splice variants of LTRPC2 identified in HL-60 cells and neutrophil granulocytes. One splice variant was activated by H_2O_2 as the wild type but did not respond to ADP-ribose, in contrast to the wild type. Thus, oxidative stress leads to the activation of LTRPC2. Channel activation, however, does not need to be directly mediated by ADP-ribose.

EXPERIMENTAL PROCEDURES

Molecular Cloning—For cloning of *LTRPC2* (formerly named TRPC7 (18)) with reverse transcriptase-polymerase chain reaction, total RNA was isolated from 1 to 2×10^7 undifferentiated HL-60 cells using TRIzol (Invitrogen, Groningen, the Netherlands). mRNA was extracted with 15 μl of Oligotex (Qiagen, Hilden, Germany). First strand cDNA synthesis was performed with 500 ng of HL-60 mRNA with Moloney murine leukemia virus reverse transcriptase (Superscript II, Invitrogen) using 500 ng of oligo(dT) primer or 2 pmol of gene-specific primer.

Two adjacent cDNA segments of *LTRPC2* that combined to the total open reading frame of *LTRPC2* were separately amplified by two PCR reactions. In the first one, primers were chosen to amplify the region between the start codon and the *Sph*I site at position 2736 (the 5′-segment coding for the N terminus of LTRPC2, 2.5 kb). In the second, the region between the mentioned *Sph*I site and the stop codon was amplified (the 3′-segment coding for the C terminus of LTRPC2, 3.2 kb). The PCR conditions were: 10 min of initial denaturation at 95 °C; 35 cycles at 95 °C for 1.5 min, 60 °C for 2 min, 72 °C for 2 min; final extension at 72 °C for 10 min. The PCR reaction mixture contained 0.4

* This work was supported by the Deutsche Forschungsgemeinschaft project B5 of Sonderforschungsbereich 542. The costs of publication of this article were defrayed in part by the payment of page charges. This article must therefore be hereby marked "*advertisement*" in accordance with 18 U.S.C. Section 1734 solely to indicate this fact.

The nucleotide sequence(s) reported in this paper has been submitted to the GenBank™/EBI Data Bank with accession number(s) AJ417076.

‡ Both authors contributed equally to this work.

§ Present address: Byk Gulden Lomberg Chemische Fabrik GmbH, Byk-Gulden-Str. 2, D-78467 Konstanz, Germany.

¶ To whom correspondence should be addressed: Institut für Physiologie, Medizinische Fakultät der RWTH Aachen, D-52057 Aachen, Germany. Tel.: 49-241-8088812; Fax: 49-241-8082434; E-mail: luckhoff@physiology.rwth-aachen.de.

[1] The abbreviations used are: LTRPC2, long transient receptor potential channel 2; TRP, transient receptor potential; $[Ca^{2+}]_i$, intracellular $[Ca^{2+}]$; EGFP, enhanced green fluorescent protein; NMDG, *N*-methyl-D-glucamine.

μM of the respective primer, 200 μM of each dNTP, 2 mM $MgCl_2$, 0.5–1 μl of cDNA and 1.25 units of *Pfu* DNA polymerase (Promega, Mannheim, Germany).

Both cDNA segments of *LTRPC2* were prepared for TA-cloning by adding adenosine tails with 1 μl of *Taq* polymerase (AmpliTaq Gold, PerkinElmer Life Sciences). Specifically, cDNA segments were dissolved in a total volume of 50 μl containing 2 mM $MgCl_2$ and 10 mM dATP and incubated at 72 °C for 30 min with the polymerase that had been preincubated in buffer at 95 °C for 10 min. Subsequently, the TA cloning (Invitrogen) was carried out.

The 5′-segment was subcloned into pBluescript SK(−) by use of the *Spe*I and *Xho*I sites of the multiple cloning site of the vector. The 3′-segment was dissected with the endonucleases *Sph*I and *Spe*I. Subsequently, ligation of the two segments was performed with T4 ligase (Invitrogen) at the *Sph*I sites of the segments and the *Spe*I site of the multiple cloning site of pBluescript SK(−).

The resulting 5.2-kb insert was directionally cloned into the eukaryotic expression plasmid construct pcDNA3-EGFP (modified as reported in Ref. 19) by use of the *Kpn*I and *Xba*I sites of the multiple cloning sites of the pcDNA3-EGFP construct. Thus, the *LTRPC2* variant is under control of the cytomegalovirus promoter, and the enhanced green fluorescent protein (EGFP) is under control of the simian virus 40 promoter.

DNA sequencing was performed with a Big-DYE terminator kit (PerkinElmer Life Sciences). A sequence alignment of our clone with *LTRPC2* (originally named TRPC7, accession number AB001535 (18)) indicated that we had obtained a variant with a deletion in the N terminus as well as in the C terminus (see Fig. 1). Additionally, several nucleotides are changed, resulting in the exchange of two amino acids (S1088N and D1292E). The details were submitted to GenBank™ under accession number AJ417076. Thus, the initial cloning yielded the *LTRPC2-ΔNΔC* form of LTRPC2 (see below, Fig. 1 and "Results").

Isolation of mRNA from Human Neutrophil Granulocytes and Demonstration of LTRPC2 Variants with Reverse Transcriptase-PCR—Venous human blood (70 ml) was taken from healthy volunteers of either sex (aged 25–35). Neutrophil granulocytes were isolated by dextran sedimentation, centrifugation through a Ficoll cushion, and separation with magnetically labeled antibodies. The isolation of total RNA (from 2.5–5 × 10^7 granulocytes) and extraction of mRNA were performed as described for HL-60 cells. For the first-strand cDNA synthesis, oligo(dT) primer were used.

For expression studies of LTRPC2 with the short and long forms of either terminus in HL-60 cells and neutrophil granulocytes, the same PCR conditions were used as described above with 0.5 μl of cDNA in a total volume of 20 μl and an annealing temperature of 63 °C (see Fig. 1 for primer sequences). Nested PCRs were performed in the same conditions as usual with 1 μl of the first PCR solution diluted 1:10.

Nomenclature—We refer to the full-length form of LTRPC2, as originally reported (18), as LTRPC2. The variant with the deletion in the N terminus (LTRPC2-Δ538–557) is named LTRPC2-ΔN. The variant with the deletion in the C terminus (LTRPC2-Δ1292–1325) is named LTRPC2-ΔC. The variant with both deletions (LTRPC2-Δ538–557, Δ1292–1325) is named LTRPC2-ΔNΔC. References to positions refer to the full-length form.

Cloning of LTRPC2 Variants for Functional Expression—Since we had initially cloned the cDNA for the LTRPC2 variant, in which the N terminus as well as the C terminus represent shortened forms of the originally described full-length form of LTRPC2, we had to insert the missing cDNA parts of either terminus to obtain the other variants. For completion of the N terminus, the following restriction sites upstream and downstream of the missing cDNA part were chosen for directional cloning: an *Xmn*I site at position 1962 and an *Sph*I site at position 2736. A segment between these sites including the missing part was amplified with three subsequent PCR reactions. The first one was designed to produce a segment starting at the *Xmn*I restriction site, extending through nucleotide 2055 of *LTRPC2* (after which the missing part starts) and additionally containing 40 nucleotides of the missing part. Accordingly, the following primers (Pa, Pb) were chosen: sense (Pa), 5′-TGTGAAGCTCTTCCTGGACG-3′; and antisense (Pb), 5′-CGCGCAACGCGGGCGCTCGGGATCCTCCACCAGCACCTTTTGCAGCTTGCT-3′. The second PCR was designed to produce a segment starting with the last 40 nucleotides of the missing part and extending to the *Sph*I restriction site. The chosen primers (Pc, Pd) were: sense (Pc), 5′-CCGAGCGCCCGGCTTGCGCGCCCGCGGCGCCCCGCCTGCACATGCACCACG-3′; and antisense (Pd), 5′-CTGCATGCACAGGGTCACACG-3′. The template for the first and second PCR was *LTRPC2-ΔN-ΔC* cloned in pBluescript SK(−). Since the missing cDNA part of the N terminus contains 60 nucleotides, there was an overlap of 20 nucleotides between the amplification products of the first and second PCR. This let these products anneal during the third PCR when they were used as templates. The primers were Pa and Pd. The idea of this PCR was that during the first cycle, both complementary strands would be elongated up to the respective restriction site and then completely amplified during the following cycles. Indeed, the PCR yielded the desired cDNA product coding for the restriction sites and for the whole part of the N terminus missing in LTRPC2-ΔNΔC. This segment was substituted for the corresponding region of the *LTRPC2-ΔNΔC* cDNA in pBluescript SK(−). The new construct corresponds to *LTRPC2-ΔC,* which was inserted into the pcDNA3-EGFP vector construct as described above.

For cloning of the *LTRPC2* cDNA constructs encoding the long form of the C terminus, a *Not*I restriction site at position 4298 was chosen. A PCR was performed with cDNA from HL-60 cells as template and the following primer pair (Pe, Pf): sense (Pe), 5′-GCGGCCGCCATGGACCCCATGGGAGACACCCTGGAGCCACTGTCCACGATCCAGTACAACGTGGTGGATGGCCTGAGGGACCGCCG-3′; and antisense (Pf), 5′-GCATACTAGTCAGTCAGTAGTGAGCCCCG-3′. Pe contains the *Not*I restriction site, the following sequence up to the missing part, and 60 nucleotides (from a total of 102 nucleotides) of the missing part. Pf contains the stop codon and an *Spe*I restriction site not present in the original *LTRPC2* gene. The amplification product with 650 bp encodes the full 3′-segment, from the *Not*I restriction site to the stop codon, and an additional *Spe*I restriction site. This product was used to create the cDNA of the *LTRPC2* variant with the complete 3′-segment coding for LTRPC2-ΔN, in pBluescript SK(−) as well as in pcDNA3-EGFP. Finally, the full-length *LTRPC2* cDNA was cloned by cutting *LTRPC2-ΔN* and *LTRPC2-ΔC* (both in pBluescript SK(−)) at the mentioned *Xba*I and *Sph*I restriction sites and subsequent ligation of the fragments coding for the long version of the N and C terminus, respectively. Insertion into pcDNA3-EGFP was performed as described above.

All PCR products were sequenced prior to further use, and all constructs were sequenced at the transition sites. All procedures were performed in accordance with the respective manufacturer's instructions, if not indicated otherwise.

Cell Culture and Transfection—Human embryonic kidney 293 (HEK 293) cells were obtained from ATCC (Manassas, VA). HEK 293 cells were cultured in Dulbecco's modified Eagle's medium (Biochrom, Berlin, Germany) supplemented with 10% (v/v) fetal calf serum (Biochrom), 1 mM sodium pyruvate (Sigma), and 4 mM L-glutamine (Biochrom). Cells were plated onto polylysine (0.1 μg/μl, Sigma)-coated glass coverslips for 24 h and then transiently transfected with one of the described pcDNA3-EGFP channel vector constructs (5 μg) and TransFast transfection reagent (7.5 μl; Promega, Mannheim, Germany). As controls, cells were transfected with 2.5 μg of "empty" vector construct and 3.75 μl of TransFast transfection reagent. Electrophysiological and fluorimetric studies were carried out 24–48 h after transfection in cells visibly positive for EGFP.

Electrophysiology—Transfected cells were studied with the patch clamp technique in the whole cell mode, using a EPC 9 equipped with a personal computer with Pulse and X chart software (HEKA, Lamprecht, Germany). The standard extracellular bath solution contained (in mM): 140 NaCl, 1.2 $MgCl_2$, 1.2 $CaCl_2$, 5 KCl, 10 HEPES, pH adjusted with KOH to 7.4. For Na^+-free solutions, Na^+ was replaced by NMDG (150 mM) and the titration was performed with HCl. For the NMDG solutions with Ca^{2+}, NMDG was partly replaced with $CaCl_2$ (11.2 mM), preserving an osmolarity of about 300 mosmol/liter. The pipette solution contained (in mM): 145 Cs-glutamate, 8 NaCl, 2 $MgCl_2$, 10 Cs-EGTA, 10 HEPES, pH 7.2 (CsOH). In some experiments, the pipette solution additionally contained ADP-ribose (0.3 mM) or NAD (final concentration of 1 mM, added to the pipette solution from a stock of 70 mM in ethanol). Cells were held at a potential of −60 mV, and current voltage (I-V) relations were obtained from voltage ramps from −90 to +60 mV applied over 400 ms.

Measurements of the Intracellular Ca^{2+} Transients—Transfected HEK 293 cells grown on poly-L-lysine-coated glass coverslips were loaded with fura-2 by incubation in fura-2 acetoxymethyl ester (2 μM, Calbiochem) for 30 min at 37 °C in a buffer consisting of (in mM): 138 NaCl, 6 KCl, 1 $MgSO_4$, 1 Na_2HPO_4, 5 $NaHCO_3$, 5.5 D-glucose, 20 HEPES, pH 7.4 (NaOH), supplemented with 0.1% (w/v) bovine serum albumin. Loaded cells were washed twice and then kept in a buffer consisting of 138 NaCl, 6 KCl, 1 $MgCl_2$, 5.5 D-glucose, 1.6 $CaCl_2$, and 20 HEPES, pH 7.4 (NaOH). Experiments were performed using a digital fluorescence imaging system (T.I.L.L. Photonics, München, Germany). Cells were visualized with a ×40 oil immersion objective (Zeiss). Emitted fluorescence was recorded after filtering through a 510-nm band pass filter over manually defined regions of interest. Excitation was performed at intervals of 2.5 s with wavelengths of 340 and 380 nm for 4 ms each, yielding the emitted fluorescence signals F_{340} and F_{380}.

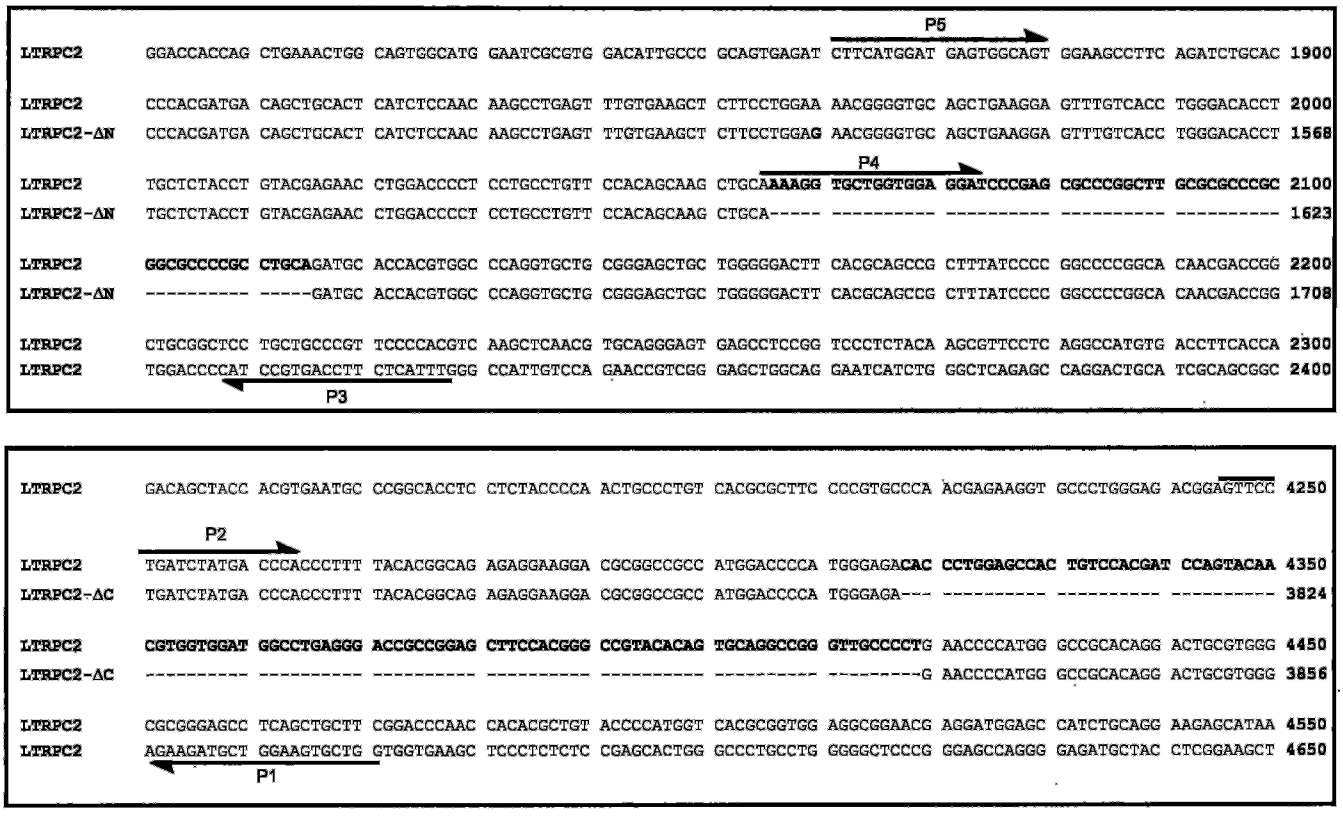

FIG. 1. **Sequence information on the splice variants of *LTRPC2* and on the primer pairs used to demonstrate expression.** The variant that we initially cloned from HL-60 cells is characterized by deletions in the 5′ (N-terminal) region (nucleotides 2056–2115) and in the 3′ (C-terminal) region (nucleotides 4318–4419). The differing sequence part within the 5′-region is aligned with that of the originally reported *LTRPC2* by Nagamine *et al.* (18) in the *top panel*. The *bottom panel* shows the respective alignment for the 3′-region. *Arrows* indicate the sequences of the forward and reverse primers used in Fig. 2. Bold letters indicate nucleotides different from the originally reported sequence of *LTRPC2*.

Bath solutions containing H_2O_2 (5–30 mM; Merck, Darmstadt, Germany) were freshly prepared daily and stored in the dark until application. Fura-2/AM was kept in a stock solution of dimethyl sulfoxide at a concentration of 1 mM stored at −20 °C until use. Unless otherwise indicated, all chemicals were purchased from Sigma. The experiments were carried out at room temperature (21–23 °C).

Data are expressed as mean ± S.D. Statistical significance between groups was assessed with the Student's *t* test. A $p < 0.05$ was considered significant.

RESULTS

Molecular Cloning of LTRPC2 and Its Variants—We cloned *LTRPC2* (formerly *LTRPC7*) from undifferentiated HL-60 cells. Initially, we obtained a clone that differs from the original sequence (18) by two deletions, from amino acids 538 to 557 and from 1292 to 1325 (Fig. 1). Additionally, two amino acids are exchanged (S1088N and D1291E). According to the structure model of TRP channels (20), the one deletion is located in the cytosolic N terminus and the other one in the cytosolic C terminus of LTRPC2. We refer to the clone with the two deletions as LTRPC2-ΔNΔC (see "Experimental Procedures"). To test whether HL-60 cells and neutrophil granulocytes express not only LTRPC2-ΔNΔC but also LTRPC2 variants with the originally reported longer forms of the N terminus and the C terminus, we performed reverse transcriptase-PCR experiments with the three primer pairs indicated in Fig. 1.

Fig. 2 shows that mRNA coding for both forms of the N terminus and for both forms of the C terminus is expressed in HL-60 cells (Fig. 2*A*) as well as in neutrophil granulocytes (Fig. 2*B*). Specifically, *lanes 1* and *4* of Fig. 2 show two different PCR products from primers P1 and P2 that demonstrate mRNA encoding the short and the long form of the C terminus. *Lanes 2* and *5* show a PCR product that can only be formed if mRNA coding for the long form of the N terminus is present. *Lanes 3* and *6* indicate the additional presence of the short form because of the size of the PCR product; note that the PCR product indicative of the long form of the N terminus is not visible in *lanes 3* and *6* but was demonstrated in a nested PCR (*lane 7*).

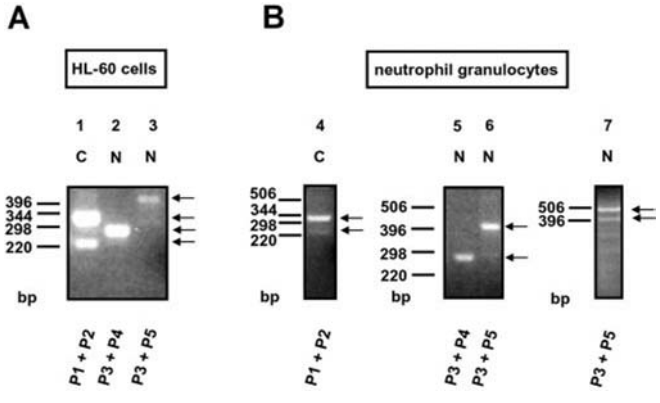

FIG. 2. **Expression of either form of the 5′ (N-terminal) and the 3′ (C-terminal) regions of *LTRPC2* mRNA in HL-60 cells (*A*) and neutrophil granulocytes (*B*).** Each *lane* shows the results of a reverse transcriptase-PCR with one pair of primers as indicated in Fig. 1. The *arrows* point to the amplificates. The expected sizes of the amplificates were: for P1/P2, 225 bp for the short form and 327 bp for the long form of the 3′ (C-terminal) fragment; P3/P4, 272 bp for the long form of the 5′ (N-terminal) fragment; and P3/P5, 406 bp for the short form and 466 bp for the long form of the 5′ (N-terminal) fragment. *Lane 7* represents a nested PCR of the experiment of *lane 6* in which the fragment with 466 bp was not demonstrated. Essentially the same results were obtained in 3–6 PCR experiments using cDNA from separate mRNA extractions. Furthermore, similar experiments with slightly modified primers (not shown) again provided evidence for the presence of mRNA encoding both variants of both termini.

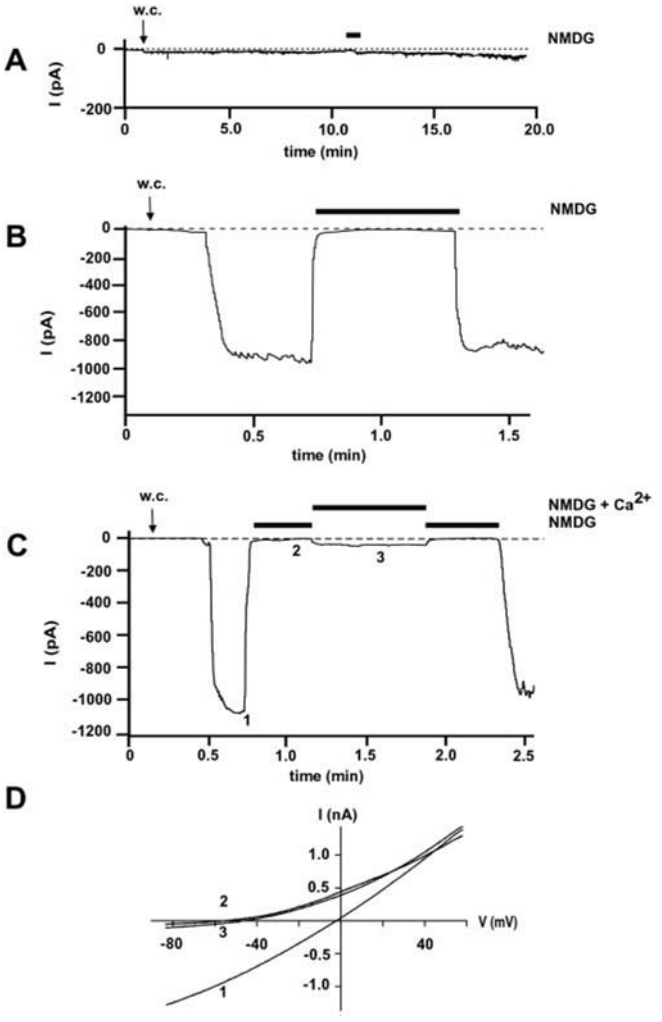

FIG. 3. **Stimulation of LTRPC2 with ADP-ribose.** *A*, original current recording from a cell expressing LTRPC2. No ADP-ribose was in the pipette solution. The whole cell configuration was obtained at the time indicated by *w.c.* The normal bath medium was exchanged for a solution with NMDG as the main cation during the time indicated by a *bar*. The holding potential was −60 mV. *B*, original current recording of one experiment in which a cell expressing LTRPC2 was patched with ADP-ribose (0.3 mM) in the pipette. *Bars* indicate times when the normal bath medium was changed to a solution with NMDG as the main cation. *C*, Ca^{2+} selectivity of LTRPC2. A cell expressing LTRPC2 and stimulated with ADP-ribose (0.3 mM in the pipette) was consecutively exposed to normal bath medium (140 mM Na^+), NMDG (150 mM, no Ca^{2+} present) bath, NMDG bath with Ca^{2+} (125 mM NMDG, 10 mM Ca^{2+}), NMDG without Ca^{2+}, and a control bath. *D*, current-voltage relationship of ADP-ribose-induced currents through LTRPC2 in the presence of various extracellular cation conditions (same experiment as in *panel C*). Voltage ramps were applied to the cells at the time points indicated with *numbers* in *panel C*.

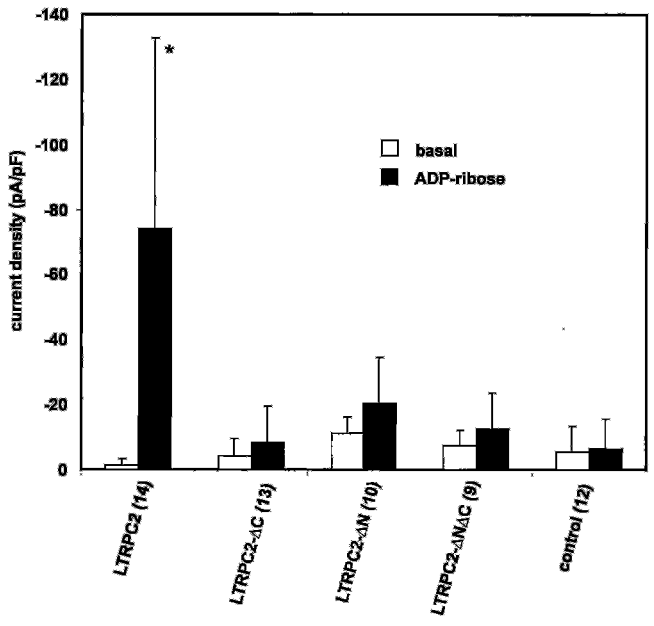

FIG. 4. **Differential stimulation of LTRPC2 variants with ADP-ribose.** For each of the four variants studied and for controls (vector-transfected cells), the initial current density (current amplitude at −60 mV, divided by the cell capacitance, a measure of cell size; *open column*) as well as the maximal current density after dialysis with ADP-ribose (0.3 mM) are displayed. At least 7 min of intracellular dialysis with ADP-ribose was allowed. The *numbers* in *parentheses* indicate the number of cells studied; significant stimulation of currents is indicated with an *asterisk*.

Sequence analysis of all the fragments shown in Fig. 2 confirmed that they represent the expected PCR products. Therefore, mRNA encoding different variants of LTRPC2 exists in HL-60 cells and neutrophil granulocytes. The HL-60 cells from which the mRNA was normally extracted were not differentiated to the granulocytic phenotype. However, mRNA coding for LTRPC2 was also demonstrated (data not shown) in HL-60 cells differentiated with dibutyryl-cAMP, a cell culture model for neutrophil granulocytes (21), but no analysis of the expressed variants was performed.

For functional studies of the LTRPC2 variants, we created four cDNA constructs coding for: (i) the full-length form of LTRPC2 with both the N terminus and the C terminus in its originally described long form; (ii) LTRPC2-ΔN (*i.e.* with the short form of the N terminus; for details, see Fig. 1 and "Experimental Procedures"); (iii) LTRPC2-ΔC; and (iv) LTRPC2-ΔNΔC. Each construct was transiently expressed in HEK 293 cells and electrophysiologically studied with the patch clamp technique in the whole cell mode.

Activation of LTRPC2 Currents by ADP-ribose—None of the expressed variants of LTRPC2 produced cation inward currents different from controls (vector-transfected cells identified by EGFP fluorescence) when the standard pipette solution was used (Fig. 3*A*). However, when ADP-ribose (0.3 mM) was present in the pipette solution in experiments with cells expressing the full-length form of LTRPC2 (Fig. 3*B*), we consistently observed an inward current that gradually developed within a few minutes after obtaining the whole cell configurations. The time elapsed before the full response to ADP-ribose occurred varied between 0.5 and 8 min. This variability is probably caused by variable diffusion times of ADP-ribose from the pipette into the cytosol and by metabolism of ADP-ribose to products that do not activate LTRPC2 (3); metabolism is expected to delay activation of LTRPC2 particularly when diffusion is already slow.

The ADP-ribose-induced inward current was abolished when extracellular Na^+ was substituted with the large impermeable cation NMDG (Fig. 3*B*). When Ca^{2+} (10 mM) was added to NMDG, a small inward current was restituted (Fig. 3, *C* and *D*). These data indicate that LTRPC2 enables non-selective cation currents carried mainly by Na^+, but to a small part also by Ca^{2+}, in the inward direction and carried by Cs^+ in the outward direction under our experimental conditions. Our results with LTRPC2 are essentially identical with those recently reported (3), where also a full-length form of LTRPC2 was used. However, when we extended the analysis to the other three forms of LTRPC2, we did not find ADP-ribose-induced currents (Fig. 4). Slightly enhanced current density levels after extended dialysis with ADP-ribose in some experiments (Fig. 4) cannot be attributed to an effect of ADP-ribose, because small

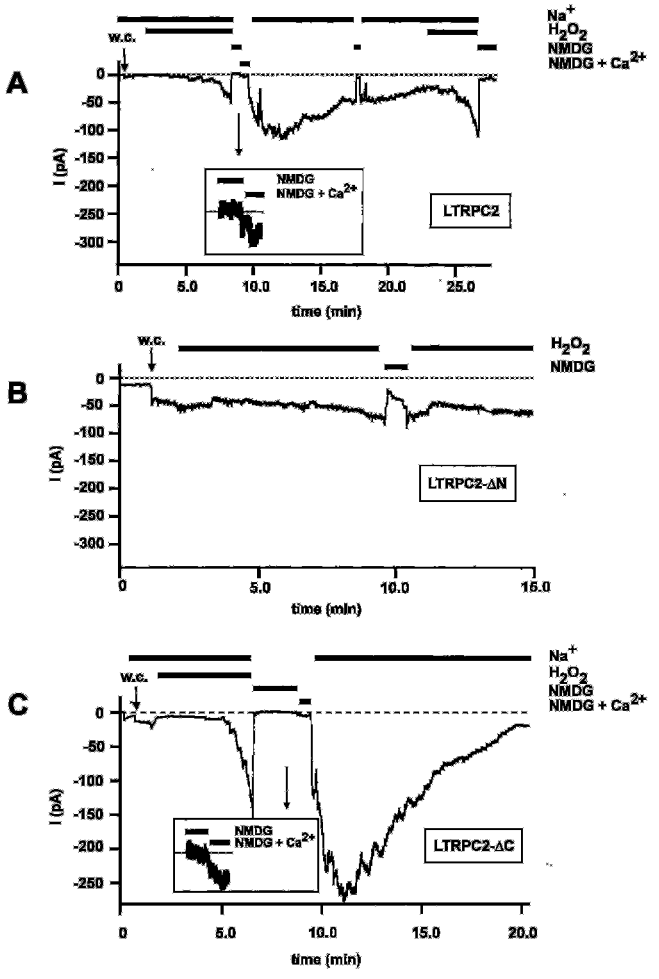

FIG. 5. **Stimulation of LTRPC2 and LTRPC2-ΔC with H_2O_2.** *A*, original current recording from one cell expressing LTRPC2. The *bars* on *top* indicate the composition of the respective bath solutions that contained Na^+, NMDG, or NMDG plus Ca^{2+} as the main cation and did or did not contain H_2O_2 (5 mM). The *inset* shows a magnification of the current tracing in NMDG solution and in NMDG solution containing additionally 11.2 mM Ca^{2+}. *B*, original current recording from one cell expressing LTRPC2-ΔN. *C*, original current recording from one cell expressing LTRPC2-ΔC.

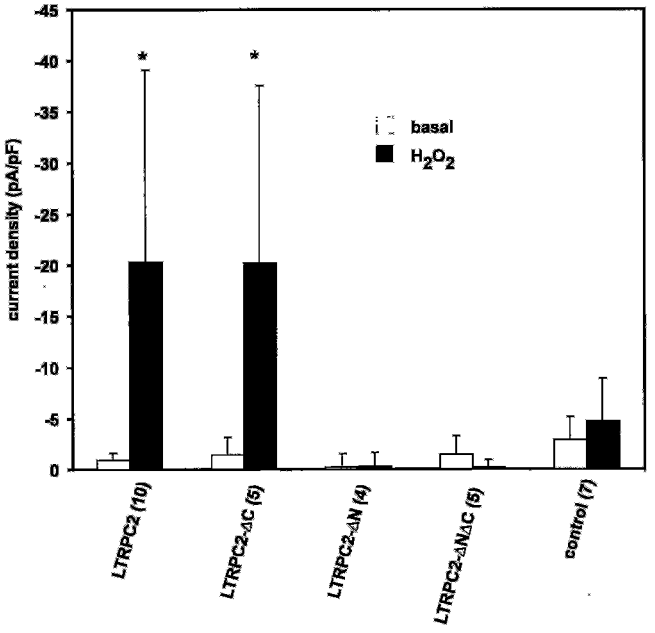

FIG. 6. **Differential stimulation of LTRPC2 splice variants with H_2O_2.** See the legend of Fig. 4 for details. The concentration of H_2O_2 was 5 or 30 mM in the bath.

current increases developed over time also in control cells in the absence of intracellular ADP-ribose (see Fig. 3*A*). Furthermore, co-transfection of cells with two vectors coding for LTRPC2-ΔC and LTRPC2-ΔN, respectively, failed to result in ADP-ribose-induced currents ($n = 4$, data not shown). Thus, stimulation with ADP-ribose was exclusively found for the full-length form of LTRPC2.

Activation of LTRPC2 Currents by Hydrogen Peroxide—As a model of oxidative stress, we tested the effects of extracellular H_2O_2 on the four LTRPC2 variants. Fig. 5*A* shows a representative experiment with a cell expressing LTRPC2 in which H_2O_2 was added to the bath to a final concentration of 5 mM. After a delay of 4 min, an inward current developed gradually that was blocked by NMDG and was partly carried by Ca^{2+}. After washout of H_2O_2, the current initially increased further but then declined almost to base-line levels, although a small NMDG-sensitive current was still present. Re-addition of H_2O_2 led to a second current rise. When the cells were exposed to H_2O_2 over more extended times than in Fig. 5, the inward currents reached a plateau after about 15 min.

Stimulation of currents with H_2O_2 after a characteristic delay was consistently observed in 10 out of 10 cells expressing LTRPC2. The mean increase in current density was from -0.9 ± 0.75 to -20.3 ± 18.8 pA/pF (Fig. 6). H_2O_2-induced increases in currents were completely abolished when the pipette solution contained the radical scavenger mannitol (10 mM). This result was obtained in 5 cells when H_2O_2 was applied for 10 min.

Although we normally used a concentration of 5 mM H_2O_2, currents were induced by H_2O_2 concentrations of 1 mM ($n = 2$) as well. Raising the H_2O_2 concentration to 30 mM resulted in current increases that were nearly irreversible over the time of the experiments, although the currents were still blocked by NMDG.

In control cells (Fig. 6) and in cells expressing either LTRPC2-ΔN (Figs. 5*B* and 6) or LTRPC2-ΔNΔC (Fig. 6), no current increase was induced by H_2O_2 (5 or 30 mM). However, in cells expressing the variant LTRPC2-ΔC that was insensitive for ADP-ribose, H_2O_2 was similarly effective (Fig. 5*C*) as in cells expressing the full-length form of LTRPC2. The currents through either form of LTRPC2 could not be discriminated by current density, time course after addition or removal of H_2O_2, or by selectivity for Ca^{2+} over Na^+ (Figs. 5*C* and 6).

Ca^{2+} Transients Induced by H_2O_2—Since the extent by which the currents through LTRPC2 were carried by Ca^{2+} was low, we studied with a different approach whether stimulation of LTRPC2 with H_2O_2 evokes increases in $[Ca^{2+}]_i$. Ca^{2+} transients in *LTRPC2*-transfected cells were followed in a digital imaging system after loading of the cells with the fluorescent Ca^{2+} indicator fura-2. After exposure to a bath containing 5 mM H_2O_2, all cells (*LTRPC2*-transfected as well as controls) responded with an initial rise in $[Ca^{2+}]_i$ (Fig. 7). $[Ca^{2+}]_i$ returned quickly to resting levels. In cells transfected with *LTRPC2* but not in control cells, a second increase in $[Ca^{2+}]_i$ was observed after several minutes (Fig. 7*B*). Such a second rise in $[Ca^{2+}]_i$ after exposure to H_2O_2 was found in 11 out of 25 *LTRPC2*-transfected cells in four independent experiments. This increase reached a plateau that remained fairly stable until the end of the experiment when further increases were elicited by ionomycin (10 μM in a buffer with 10 mM Ca^{2+}). However, a calibration of the fluorescence signal in terms of Ca^{2+} concentration was not done because many cells detached during the long time required for experiments with H_2O_2.

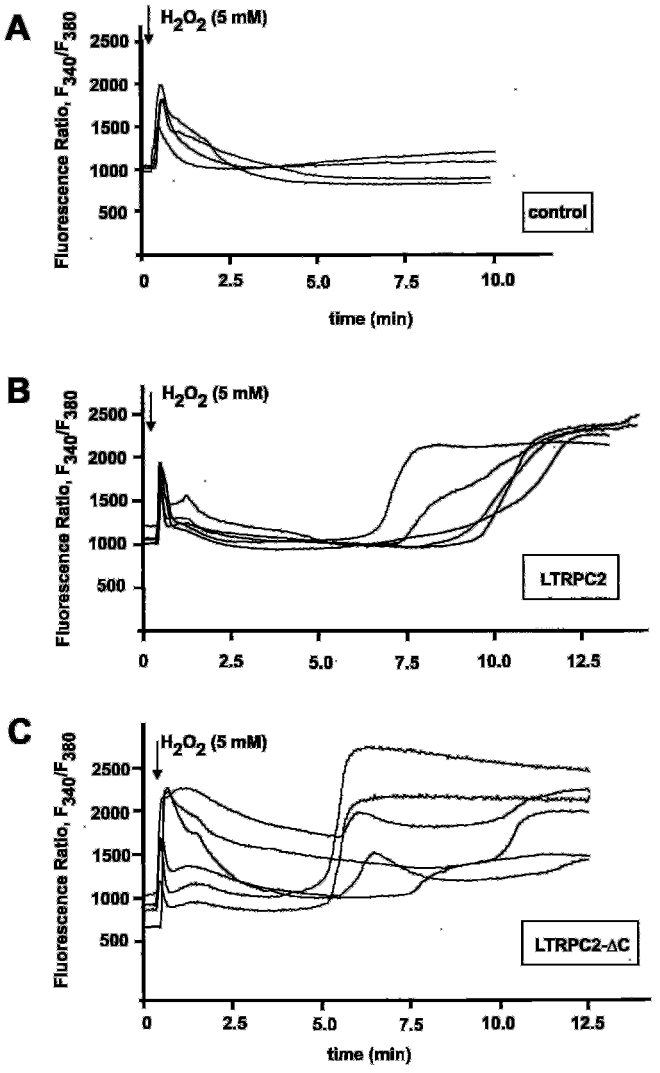

FIG. 7. **Effects of H_2O_2 on Ca^{2+} transients in *LTRPC2*-transfected and control cells.** *A*, original tracings obtained from six representative control cells. The ratio of F_{340} to F_{380} was followed over time. H_2O_2 (bath concentration, 5 mM) was applied at the time indicated by the *arrow*. *B*, original tracings from five representative cells transfected with *LTRPC2*. *C*, original tracings from six representative cells transfected with *LTRPC2*-Δ*C*.

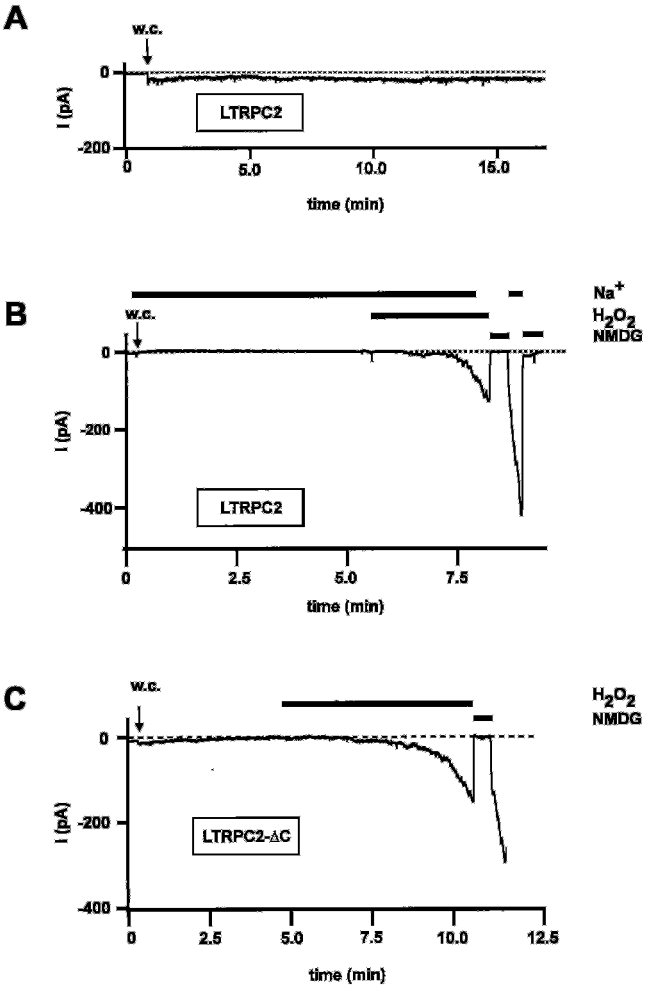

FIG. 8. **Comparison of the effects of NAD and H_2O_2 on LTRPC2.** *A*, current recording from a cell expressing LTRPC2 with NAD (1 mM) in the pipette. *B*, current recording from a cell expressing LTRPC2 with NAD (1 mM) in the pipette. A time of 300 s after obtaining the whole cell configuration was allowed before a stimulation with H_2O_2 (5 mM) was performed. *C*, current recording from a cell expressing LTRPC2-ΔC with ADP-ribose (0.3 mM) in the pipette. A time of 300 s after obtaining the whole cell configuration was allowed before stimulation with H_2O_2 (5 mM) was performed.

No H_2O_2-induced second rise in $[Ca^{2+}]_i$ was seen in any control cells (n = 23 in four experiments). Likewise, no such rise was seen in *LTRPC2*-transfected cells in the absence of H_2O_2 (n = 19 in four experiments).

Similar results as with the full-length LTRPC2 were obtained with LTRPC2-ΔC (Fig. 7*C*). Here, the second rise in $[Ca^{2+}]_i$ occurred in 17 out of 41 *LTRPC2*-Δ*C*-transfected cells in five experiments and not in any control cell (n = 9).

Lack of LTRPC2 Activation by NAD—As LTRPC2 has been reported to be stimulated by intracellular NAD (16), we also tested this compound which was applied to the cells by dialysis through the patch pipette. However, LTRPC2 did not respond to NAD with an increase in currents (Fig. 8*A*; n = 7). These negative findings were confirmed with the other three forms of LTRPC2 and in controls (n = 4–5). To demonstrate that the lack of NAD effects was not a problem of LTRPC2 expression, we applied H_2O_2 (5 mM) to cells that had been dialyzed with NAD for 5 min without showing any indication of a developing current. After a further delay of 2 min, a gradually increasing current was observed (Fig. 8*B*). Essentially the same finding as in cells expressing LTRPC2 was obtained in cells expressing LTRPC2-ΔC (n = 2). Thus, stimulation with H_2O_2 was independent of the presence of NAD in the pipette solution, whereas NAD alone did not stimulate currents through LTRPC2.

Differential Sensitivity of LTRPC2-ΔC for H_2O_2 and ADP-ribose—Furthermore, we tested whether stimulation by H_2O_2 was independent of ADP-ribose (Fig. 8*C*). Cells expressing LTRPC2-ΔC were patched with ADP-ribose (0.3 mM) present in the pipette solution. A time of 5 min was allowed during which ADP-ribose failed to induce currents, as in the previous experiments (Fig. 4). Then, H_2O_2 was applied extracellularly. Again, after a delay of 2 min, the typical H_2O_2-induced currents were observed (n = 3) that were slowly increasing and blocked by the impermeable cation NMDG (Fig. 8*C*).

DISCUSSION

The present study found that the non-selective cation channel LTRPC2 was activated by H_2O_2. This is a alternative mode of activation for this channel that has previously been demonstrated to be activated by ADP-ribose (3). A splice variant of LTRPC2, LTRPC2-ΔC, identified in HL-60 cells and in neutrophil granulocytes, was differentially sensitive for the two stimuli because it was exclusively activated by H_2O_2. Thus,

LTRPC2-ΔC reveals some information on the structural requirements for ADP-ribose sensitivity and provides evidence that both stimuli act by distinct mechanisms.

NAD has recently been reported to stimulate LTRPC2 (16, 17). However, we did not see activation of any form of LTRPC2 by NAD, which does not support the idea that this substance activates LTRPC2 directly. Since ADP-ribose is a metabolite of NAD (13, 14), it is conceivable that NAD is converted to ADP-ribose under some experimental conditions to a sufficient extent to stimulate LTRPC2; however, this may depend on very subtle details and obviously did not occur in our experiments.

When we started the functional characterization of LTRPC2, we reasoned that both NAD and ADP-ribose may be mediators of oxidative stress because the intracellular concentrations of NAD and, consequently, of ADP-ribose may be increased when the redox potential of the cell is altered such that the equilibrium of NAD to NADH is shifted in favor of NAD. The same phenomenon is expected to occur whenever a strong membrane-permeant oxidant such as H_2O_2 is applied. Indeed, H_2O_2 induced a consistent activation of LTRPC2, even though the amplitude of the resulting currents was lower than under stimulation with ADP-ribose. The stimulation by H_2O_2 was prevented by intracellular mannitol, a radical scavenger (22), suggesting that H_2O_2 acts by generation of free radicals in the cell interior. However, the experiments with LTRPC2-ΔC are not in line with our original hypothesis that the effects of oxidative stress are mediated by ADP-ribose because this compound proved ineffective on this splice variant of LTRPC2, in distinct contrast to H_2O_2 that activated LTRPC2-ΔC to the same extent as wild-type LTRPC2. Therefore, it appears that oxidative stress can stimulate LTRPC2 by different mechanisms, either mediated by or independent of ADP-ribose.

The various variants of LTRPC2, characterized by deletions of 20 or 34 amino acids in the N terminus and C terminus of the channel, provide information on structural requirements for the channel function of LTRPC2. The deletion in the C terminus that abolished the effects of ADP-ribose is distant from the Nudix box. Therefore, the presence of a Nudix box alone is not sufficient to predict ADP-ribose sensitivity of a channel. On the contrary, subtle additional structural details decide whether channels are sensitive or completely insensitive for ADP-ribose. The N-terminal deletion prevented the response to both ADP-ribose and H_2O_2. The variants with the short form of the N terminus may not even form functional ion channels. Alternatively, they may be used to control the expression of the other variants, as has been reported for partial sequences of another member of the TRP family, TRPM4 (23).

Our study suggests that LTRPC2 in both its active forms plays an important role in various tissues because it enables Ca^{2+} influx in response to oxidants. The consequences of oxidative stress are not confined to nonselective cell damage by mechanisms like lipid peroxidation. Evidence has been provided that specific cellular responses are induced, including activation of transcription factors like the nuclear factor-κB and the activator protein-1, phospholipase D, the p38 mitogen-activated protein kinase pathway, or receptor tyrosine kinases (24–27). Ca^{2+} has been attributed an important function for many of these processes (28, 29). Thus, activation of the Ca^{2+}-permeable channel LTRPC2 may be a distinct mechanism by which specific cells are capable of reacting to damaging oxidants. It is noteworthy that cation channels with similar biophysical properties (30) as LTRPC2 (3) were activated by H_2O_2 in an insulin-secreting pancreatic cell line. H_2O_2 altered the redox state of the cells and mimicked the diabetes-inducing toxic effects of alloxan.

The role of oxidant-mediated activation of LTRPC2 may be of particular relevance for neutrophil granulocytes in which we have demonstrated expression of *LTRPC2*. One of the characteristic responses of these cells after activation by chemokines is the respiratory burst during which superoxide anions and other free radicals are generated at high concentrations (31). Since depolarization and increases in $[Ca^{2+}]_i$ are among the key responses of neutrophil granulocytes to chemokines (32–34), an H_2O_2-sensitive pathway for Na^+ and Ca^{2+} represents part of a positive feedback loop leading to massive cation influx and Ca^{2+} load during the respiratory burst.

In conclusion, the present study demonstrates activation of the cation channel LTRPC2 by H_2O_2, leading to influx of Na^+ and Ca^{2+} into LTRPC2-expressing cells. A splice variant found in neutrophil granulocytes with a deletion in the C terminus demonstrates that H_2O_2 uses a different mode of channel activation than ADP-ribose. Thus, LTRPC2 represents a cation channel that links the redox state of the cell to Ca^{2+} homeostasis, as has also been reported by Hara *et al.* (17) after submission of our manuscript.

Acknowledgment—We thank Ilinca Ionescu for expert technical assistance.

REFERENCES

1. Harteneck, C., Plant, T. D., and Schultz, G. (2000) *Trends Neurosci.* **23,** 159–166
2. Runnels, L. W., Yue, L., and Clapham, D. E. (2001) *Science* **291,** 1043–1047
3. Perraud, A. L., Fleig, A., Dunn, C. A., Bagley, L. A., Launay, P., Schmitz, C., Stokes, A. J., Zhu, Q., Bessman, M. J., Penner, R., Kinet, J. P., and Scharenberg, A. M. (2001) *Nature* **411,** 595–599
4. Bessman, M. J., Frick, D. N., and O'Handley, S. F. (1996) *J. Biol. Chem.* **271,** 25059–25062
5. Howard, M., Grimaldi, J. C., Bazan, J. F., Lund, F. E., Santos-Argumedo, L., Parkhouse, R. M., Walseth, T. F., and Lee, H. C. (1993) *Science* **262,** 1056–1059
6. Lee, H. C., and Aarhus, R. (1993) *Biochim. Biophys. Acta* **1164,** 68–74
7. Takasawa, S., Tohgo, A., Noguchi, N., Koguma, T., Nata, K., Sugimoto, T., Yonekura, H., and Okamoto, H. (1993) *J. Biol. Chem.* **268,** 26052–26054
8. Cancela, J. M., Gerasimenko, O. V., Gerasimenko, J. V., Tepikin, A. V., and Petersen, O. H. (2000) *EMBO J.* **19,** 2549–2557
9. Clementi, E., Riccio, M., Sciorati, C., Nistico, G., and Meldolesi, J. (1996) *J. Biol. Chem.* **271,** 17739–17745
10. Galione, A., Lee, H. C., and Busa, W. B. (1991) *Science* **253,** 1143–1146
11. Meszaros, L. G., Bak, J., and Chu, A. (1993) *Nature* **364,** 76–79
12. Sonnleitner, A., Conti, A., Bertocchini, F., Schindler, H., and Sorrentino, V. (1998) *EMBO J.* **17,** 2790–2798
13. Berthelier, V., Tixier, J. M., Muller-Steffner, H., Schuber, F., and Deterre, P. (1998) *Biochem. J.* **330,** 1383–1390
14. Ziegler, M. (2000) *Eur. J. Biochem.* **267,** 1550–1564
15. Wilson, H. L., Dipp, M., Thomas, J. M., Lad, C., Galione, A., and Evans, A. M. (2001) *J. Biol. Chem.* **276,** 11180–11188
16. Sano, Y., Inamura, K., Miyake, A., Mochizuki, S., Yokoi, H., Matsushime, H., and Furuichi, K. (2001) *Science* **293,** 1327–1330
17. Hara, Y., Wakamori, M., Ishii, M., Maeno, E., Nishida, M., Yoshida, T., Yamada, H., Shimizu, S., Mori, E., Kudoh, J., Shimizu, N., Kurose, H., Okada, Y., Imoto, K., and Mori, Y. (2002) *Mol. Cell* **9,** 163–173
18. Nagamine, K., Kudoh, J., Minoshima, S., Kawasaki, K., Asakawa, S., Ito, F., and Shimizu, N. (1998) *Genomics* **54,** 124–131
19. Halaszovich, C. R., Zitt, C., Jüngling, E., and Lückhoff, A. (2000) *J. Biol. Chem.* **275,** 37423–37428
20. Hardie, R. C., and Minke, B. (1992) *Neuron* **8,** 643–651
21. Collins, S. J. (1987) *Blood* **70,** 1233–1244
22. Suzuki, J., Imaizumi, S., Kayama, T., and Yoshimoto, T. (1985) *Stroke* **16,** 695–700
23. Xu, X. Z., Moebius, F., Gill, D. L., and Montell, C. (2001) *Proc. Natl. Acad. Sci. U. S. A.* **98,** 10692–10697
24. Knebel, A., Rahmsdorf, H. J., Ullrich, A., and Herrlich, P. (1996) *EMBO J.* **15,** 5314–5325
25. Meyer, M., Schreck, R., and Baeuerle, P. A. (1993) *EMBO J.* **12,** 2005–2015
26. Schreck, R., Rieber, P., and Baeuerle, P. A. (1991) *EMBO J.* **10,** 2247–2258
27. Thannickal, V. J., and Fanburg, B. L. (2000) *Am. J. Physiol.* **279,** L1005–L1028
28. Conrad, P. W., Millhorn, D. E., and Beitner-Johnson, D. (2000) *Adv. Exp. Med. Biol.* **475,** 293–302
29. Ito, Y., Nakashima, S., and Nozawa, Y. (1997) *J. Neurochem.* **69,** 729–736
30. Herson, P. S., and Ashford, M. L. (1997) *J. Physiol. (Lond.)* **501,** 59–66
31. Cohen, M. S. (1994) *Clin. Infect. Dis.* **18,** Suppl. 2, S170–S179
32. Krause, K. H., Demaurex, N., Jaconi, M., and Lew, D. P. (1993) *Blood Cells* **19,** 165–173
33. Schorr, W., Swandulla, D., and Zeilhofer, H. U. (1999) *Eur. J. Immunol.* **29,** 897–904
34. Walz, A., Meloni, F., Clark-Lewis, I., von Tscharner, V., and Baggiolini, M. (1991) *J. Leukocyte Biol.* **50,** 279–286